

Article

Water Stress Alters Physiological, Spectral, and Agronomic Indexes of Wheat Genotypes

Cássio Jardim Tavares ¹, Walter Quadros Ribeiro Junior ^{2,*}, Maria Lucrecia Gerosa Ramos ^{3,*},
Lucas Felisberto Pereira ⁴, Onno Muller ⁵, Raphael Augusto das Chagas Noqueli Casari ⁶,
Carlos Antonio Ferreira de Sousa ⁷ and Anderson Rodrigo da Silva ⁸

- ¹ Federal Institute Goiano, Campus Cristalina (IF Goiano), Cristalina 73850-000, GO, Brazil; cassio.tavares@ifgoiano.edu.br
- ² Brazilian Agricultural Research Corporation—(EMBRAPA Cerrados), Planaltina 73310-970, DF, Brazil
- ³ Faculty of Agronomy and Veterinary Medicine, University of Brasília, Brasília 70910-900, DF, Brazil
- ⁴ Federal Institute Goiano, Campus Posse (IF Goiano), Posse 73900-000, GO, Brazil; lucas.felisberto@ifgoiano.edu.br
- ⁵ Institute for Bio-and Geosciences, IBG-2: Plant Sciences, Forschungszentrum Jülich GmbH, 52428 Jülich, Germany; o.muller@fz-juelich.de
- ⁶ Institute of Geosciences, University of Brasília, Brasília 70910970, DF, Brazil; casari.raphael@gmail.com
- ⁷ Brazilian Agricultural Research Corporation—(EMBRAPA Meio-Norte), Teresina 64008-780, PI, Brazil; carlos.antonio@embrapa.br
- ⁸ Federal Institute Goiano, Campus Urutaí (IF Goiano), Urutaí 75790-000, GO, Brazil; anderson.silva@ifgoiano.edu.br
- * Correspondence: walter.quadros@embrapa.br (W.Q.R.J.); lucreciaunb@gmail.com (M.L.G.R.)

Abstract: Selecting drought-tolerant and more water-efficient wheat genotypes is a research priority, specifically in regions with irregular rainfall or areas where climate change is expected to result in reduced water availability. The objective of this work was to use high-throughput measurements with morphophysiological traits to characterize wheat genotypes in relation to water stress. Field experiments were conducted from May to September 2018 and 2019, using a sprinkler bar irrigation system to control water availability to eighteen wheat genotypes: BRS 254; BRS 264; CPAC 01019; CPAC 01047; CPAC 07258; CPAC 08318; CPAC 9110; BRS 394 (irrigated biotypes), and Aliança; BR 18_Terena; BRS 404; MGS Brilhante; PF 020037; PF 020062; PF 120337; PF 100368; PF 080492; and TBIO Sintonia (rainfed biotypes). The water regimes varied from 22 to 100% of the crop evapotranspiration replacement. Water stress negatively affected gas exchange, vegetation indices, and grain yield. High throughput variables TCARI, NDVI, OSAVI, SAVI, PRI, NDRE, and GNDVI had higher yield and morphophysiological measurement correlations. The drought resistance index indicated that genotypes Aliança, BRS 254, BRS 404, CPAC 01019, PF 020062, and PF 080492 were more drought tolerant.

Keywords: automation; *Triticum aestivum*; gas exchange; drought tolerance; high throughput; Cerrado



Citation: Tavares, C.J.; Ribeiro Junior, W.Q.; Ramos, M.L.G.; Pereira, L.F.; Muller, O.; Casari, R.A.d.C.N.; de Sousa, C.A.F.; da Silva, A.R. Water Stress Alters Physiological, Spectral, and Agronomic Indexes of Wheat Genotypes. *Plants* **2023**, *12*, 3571. <https://doi.org/10.3390/plants12203571>

Academic Editors: Beata Dedicova and Jagdish Rane

Received: 14 September 2023

Revised: 7 October 2023

Accepted: 12 October 2023

Published: 14 October 2023



Copyright: © 2023 by the authors. Licensee MDPI, Basel, Switzerland. This article is an open access article distributed under the terms and conditions of the Creative Commons Attribution (CC BY) license (<https://creativecommons.org/licenses/by/4.0/>).

1. Introduction

Brazil has an annual demand of about 12 million tons of wheat grains, producing less than half of its needs and importing the other part [1]. Therefore, looking for alternatives to increase crop productivity and include new areas to reduce foreign dependence and expenditure on wheat imports is important.

Cerrado is a vast savanna biome in the Brazilian highlands and has been an alternative for rainfed or irrigated wheat cultivation [2], as it has favorable climatic and soil conditions. During winter in the Cerrado region, wheat has high yields under irrigation conditions and should be efficient in water use. In contrast, when planting wheat in the off-season, during the summer, the main limitation is dry periods, which require drought-tolerant plants [2].

Wheat cultivation during the summer (early crop) depends on the previous crop cycle, considering drought escape, water availability, drought-tolerant cultivars, and diseases such as blast (*Pyricularia oryzae*), which are the main limiting factors for wheat cultivation in the off-season [3].

However, in rainfed (off-season) cultivation, irregular rainfall and prolonged dry periods (dry spells) [4] are common in this region. Among the environmental changes that affect crop development, the ones caused by the water deficit, which intensified in recent years due to global warming [5,6], stand out.

A reduction in precipitation in the critical stages of crop development has been reported, especially in the Brazilian Cerrado, one of the largest grain producers in the country [7], with drastic reductions in crop productivity [8]. In this scenario, understanding the mechanisms plants use to tolerate water stress is crucial to identifying wheat cultivars with tolerance and/or water-use efficiency, consequently decreasing the productivity and grain quality losses of these crops.

Drought can be minimized through proper management [9] and genetic tolerance. To unravel genetic tolerance, it is necessary to identify genotypes that minimally reduce their yield potential and grain quality under conditions of low water availability [1].

The survival of plants under drought depends on several mechanisms acting simultaneously: reduction of the growing cycle, stomatal opening and transpiration rate, and the development of antioxidants that maintain osmotic adjustments at the tissue level [10]. Consequently, morphophysiological and crop yield changes may occur [11].

Because of the water deficit effects on plants, genotypes tolerant to water stress can be identified by combining several variables, namely drought tolerance indices [2], water-use efficiency [12], productivity components [13], physiological index [14,15], and vegetation (spectral) indices [16,17], and these variables may be correlated with grain yield and quality [18]. The effect of stomatal closure is a reduction in photosynthesis, but screening based on photosynthetic parameters or stomatal conductance measurements is generally slow [19].

New technologies and methodologies that measure these variables should offer advantages in relation to yield levels, applicability in field conditions (in various climatic conditions), and speed in obtaining this information. The use of tools that provide a rapid assessment and are non-invasive and destructive at any stage of crop development and with high precision on the characteristics of plants in relation to abiotic and biotic factors has been used in the studies of the interaction plant environment [20].

A phenotyping platform for field drought tolerance was developed and used at Embrapa Cerrados as described by Jayme-Oliveira [21] for several annual and perennial species. Automated watering systems, often integrated with high-throughput phenotyping tools, are critical to experimentation, as a manual water application is imprecise and labor-intensive [22].

Among these tools, using sensors in agriculture can provide valuable information on plant physiology under water stress by detecting changes related to plant structure, pigments, and photosynthetic efficiency [23].

Using sensors coupled on land platforms [24] or unmanned aerial vehicles [25] has the advantage of a rapid, non-destructive evaluation with high precision. However, there is a need to validate the efficiency of these tools. Among these sensors, multispectral cameras are coupled in unmanned vehicles, which can be used to select cultivars adapted to different conditions [26], an indispensable tool in breeding programs.

Thus, multispectral sensors that capture wavelengths in the visible and near-infrared range of the electromagnetic spectrum allow the calculation of various vegetation indices [20] and can be used for rapid and non-destructive selection of drought-tolerant wheat genotypes [27] with high precision [28]. Multispectral traits derived from NIR, red, and green bands showed a strong relationship with wheat biomass, water-use efficiency, photosynthesis, and grain yield. The study of morphophysiological, spectral, and produc-

tivity changes due to water stress in wheat genotypes is important for selecting cultivars that are more tolerant to water stress [17].

Therefore, the characterization of genotypes tolerant to water stress in rainfed cultivation and greater water-use efficiency in irrigated cultivation under Cerrado [2] conditions is important to increase grain yield and quality. This work hypothesizes that non-destructive physiological responses of wheat, as well as high throughput vegetative indices, are related to soil water availability and can be used to discriminate tolerant genotypes to water stress. Thus, this work aimed to validate the use of sensors as a tool for selecting wheat genotypes for drought tolerance through morphophysiological and agronomic assessments under field conditions.

2. Results

Variable Contributions in the Multivariate Response

Data were submitted to joint multivariate analysis of variance, and significant differences were found for the sources of variation genotypes ($p < 0.01$), water regime ($p < 0.01$), year of cultivation ($p < 0.01$), and the interaction genotypes \times water regime ($p < 0.01$) (Table 1). However, there was no significant ($p > 0.05$) effect of the interaction genotype \times water regime \times cropping year ($p = 1$). The significance of genotype \times water regime interaction shows that genotypes respond differently to water availability.

Table 1. Summary of the multivariate analysis of variance (MANOVA) joined with all interactions.

Source	Df	Pillai	Approx F	Num Df	Den Df	Probability
Year	1	0.882	44.831	31	186	2.2×10^{-16} **
Genotypes	17	6.5224	4.056	527	3434	2.2×10^{-16} **
Water regime	3	2.6453	45.234	93	564	2.2×10^{-16} **
Year:Block	4	2.2584	7.906	124	756	2.2×10^{-16} **
Year:Genotypes	17	1.6662	0.708	527	3434	1 ^{ns}
Year:Water regime	3	0.9002	2.600	93	564	7.026×10^{-12} **
Genotypes:Water regime	51	9.6958	1.928	1581	564	2.2×10^{-16} **
Year:Block:Genotypes	68	9.9413	1.500	2108	6699	2.2×10^{-16} **
Year:Genotypes:Water regime	51	1.8329	0.266	1581	6699	1 ^{ns}
Residuals	216					

** $p < 0.01$; ns: not significant.

After a joint multivariate statistical analysis, the wheat genotypes were grouped in Group 1: Aliança, BRS 254, BRS 404, CPAC 01019, PF 020062, and PF 080492; Group 2: BR 18_Terena, MGS Brilhante, PF 020037, and PF 120337; Group 3: BRS 264, BRS 394, CPAC 01047, CPAC 07258, CPAC 8318, CPAC 9110, PF 100368, and TBIO Sintonia. The average values of the variables analyzed in the wheat crop according to the groups of genotypes and water regimes in 2018 and 2019 are presented in Tables 2 and 3. In general, changes in water availability affected the morphophysiological and spectral characteristics and crop yield, with different levels in the genotypes studied.

Table 2. Mean values of vegetative indices and wheat yield according to the groups of genotypes and water regimes in the 2018 and 2019 cropping years.

G ^{1/}	WR	Variables												
		NDVI	SAVI	PRI	DVI	GRVI	GNDVI	NDRE	TCARI	OSAVI	TO	GH	MTG	GY
1	22	0.27	0.18	0.1	1.81	3.09	0.5	0.12	0.12	0.22	0.54	10.5	32.97	2337
	43	0.45	0.28	0.16	3.17	3.89	0.58	0.25	0.14	0.36	0.4	10.8	35.19	3691
	81	0.62	0.38	0.21	5.58	4.7	0.63	0.34	0.18	0.49	0.38	11.3	37.56	5076
	100	0.65	0.39	0.22	6.27	5.06	0.65	0.35	0.18	0.51	0.37	11.4	38.74	5604

Table 2. Cont.

G ^{1/}	WR	Variables												
		NDVI	SAVI	PRI	DVI	GRVI	GNDVI	NDRE	TCARI	OSAVI	TO	GH	MTG	GY
2	22	0.29	0.19	0.12	1.93	3.15	0.51	0.14	0.12	0.24	0.54	11.2	33.68	1983
	43	0.47	0.3	0.17	3.38	3.97	0.58	0.26	0.15	0.38	0.41	10.9	36.2	3913
	81	0.63	0.39	0.23	5.91	4.82	0.63	0.35	0.18	0.5	0.37	11.6	36.99	5095
	100	0.65	0.41	0.23	6.6	5.2	0.66	0.37	0.18	0.52	0.36	11.8	38.43	5439
3	22	0.24	0.16	0.09	1.67	2.93	0.49	0.11	0.11	0.2	0.55	10.3	32.43	2366
	43	0.4	0.24	0.14	2.56	3.51	0.55	0.21	0.13	0.31	0.43	10.3	36.31	4013
	81	0.6	0.37	0.21	5.04	4.38	0.61	0.31	0.19	0.47	0.4	10.6	39.97	5653
	100	0.64	0.39	0.22	6.04	4.86	0.64	0.33	0.19	0.51	0.39	10.8	40.43	6052
Mean		0.49	0.31	0.17	4.16	4.13	0.59	0.26	0.16	0.39	0.43	10.9	36.57	4269
SE		0.05	0.03	0.01	0.55	0.24	0.02	0.03	0.01	0.04	0.02	0.15	0.76	414.5
CV		3.28	3.1	2.97	4.62	1.98	1.03	3.67	2.02	3.19	1.66	0.46	0.72	3.36

G^{1/}: groups of genotypes; WR: water regimes (22, 43, 81, and 100% CET—WR1, WR2, WR3 and WR4, respectively); NDVI: normalized difference vegetation index; SAVI: soil-adjusted vegetation index; PRI: photochemical-physiological reflectance index; DVI: difference vegetation index; GRVI: green-red vegetation index; GNDVI: green normalized difference vegetation index; NDRE: normalized difference red edge; TCARI: chlorophyll absorption and reflectance index; OSAVI: optimized soil-adjusted vegetation index; TO: TCARI/OSAVI; GH: grain humidity (%); MTG: mass of thousand grains (g); GY: grain yield (Kg.ha⁻¹). Group 1: Aliança, BRS 254, BRS 404, CPAC 01019, PF 020062, and PF 080492; Group 2: BR 18_Terena, MGS Brilhante, PF 020037, and PF 120337; Group 3: BRS 264, BRS 394, CPAC 01047, CPAC 07258, CPAC 8318, CPAC 9110, PF 100368, and TBIO Sintonia. SE: standard error; CV: coefficient of variation (%).

Table 3. Mean values morphophysiological and drought tolerance index of wheat according to the groups of genotypes and water regimes in the 2018 and 2019 cropping years.

G ^{1/}	WR	Variables													
		WUE	Cha	Chb	RM	SM	A	gs	iWUE	Ci	E	Fv'/Fm'	ETR	Fv/Fm	DRI
1	22	22.7	30.9	7.2	4.9	10.4	8.7	0.09	121.9	188	2.5	0.46	122	0.8	1.01
	43	19.5	35.5	10.5	5	12.2	15.8	0.13	96.8	204	3.2	0.5	144	0.82	
	81	14.3	39.4	14.1	5.8	15.7	22.3	0.33	67.8	248	6.3	0.57	148	0.82	
	100	12.5	41.0	16.0	5.7	15.6	22.7	0.48	47.2	275	8.7	0.59	151	0.83	
2	22	20.3	32.0	8.2	5.4	11.1	9.7	0.09	125.6	193	2.5	0.47	133	0.81	0.95
	43	19.1	35.3	11.4	9.8	12.9	15.1	0.12	108.4	175	3.2	0.51	146	0.83	
	81	14.1	40.2	16.1	6.1	13.6	21.6	0.39	55.5	263	7.8	0.6	150	0.83	
	100	12.2	41.6	16.7	5.6	15.2	22.1	0.53	41.8	273	9.9	0.6	164	0.83	
3	22	22.0	27.4	5.4	4.8	9.9	8.1	0.09	127.1	168	2.6	0.4	99	0.8	0.93
	43	20.3	32.6	8.2	5.1	11.6	16.0	0.1	112.0	144	2.9	0.5	116	0.81	
	81	16.0	38.6	13	5.2	15.7	23.1	0.41	56.4	259.9	7.68	0.6	159	0.82	
	100	13.6	40.2	14.2	5.5	17.1	23.9	0.61	49.3	294.9	11.55	0.6	142	0.83	
Mean		17.2	36.1	11.7	5.7	13.4	17.4	0.28	84.1	224.2	5.75	0.5	140	0.82	0.96
SE		1.1	1.34	1.1	0.4	0.7	1.7	0.06	4.87	14.56	0.96	0.02	5.49	0.09	0.01
CV		2.2	1.28	3.3	2.3	1.8	3.4	7.05	1.12	2.25	5.77	1.29	1.36	0.13	0.11

G^{1/}: group of genotypes; WR: water regimes (22, 43, 81, and 100% CET—WR1, WR2, WR3 and WR4, respectively); WUE: water-use efficiency; Cha: chlorophyll a; Chb: chlorophyll b; RM: root mass; SM: shoot mass; A: net assimilation of CO₂ (μmol CO₂ m⁻² s⁻¹); gs: stomatal conductance (mol H₂O m⁻² s⁻¹); iWUE: intrinsic water-use efficiency (iWUE—A/gs: net assimilation of CO₂/stomatal conductance); Ci: internal CO₂ concentration (ppm); E: transpiration (mmol H₂O m⁻² s⁻¹); Fv'/Fm': effective quantum yield of photosystem II; ETR: electron transport rate; Fv/Fm: maximum quantum yield of photosystem II. DRI: drought resistance index. Group 1: Aliança, BRS 254, BRS 404, CPAC 01019, PF 020062, and PF 080492; Group 2: BR 18_Terena, MGS Brilhante, PF 020037, and PF 120337; Group 3: BRS 264, BRS 394, CPAC 01047, CPAC 07258, CPAC 8318, CPAC 9110, PF 100368, and TBIO Sintonia. SE: standard error; CV: coefficient of variation (%).

In Figure 1, three groups of genotypes were identified. Group 1 with six genotypes (33.33%) (Aliança; BRS 254; BRS 404; CPAC 01019; PF 020062; and PF 080492); Group 2 has four genotypes (22.22%) (BR 18_Terena; MGS Brilhante; PF 020037; and PF 120337) and

Group 3 has eight genotypes (44.45%) (BRS 264; BRS 394; CPAC 01047; CPAC 07258; CPAC 8318; CPAC 9110; PF 100368; and TBIO Sintonia).

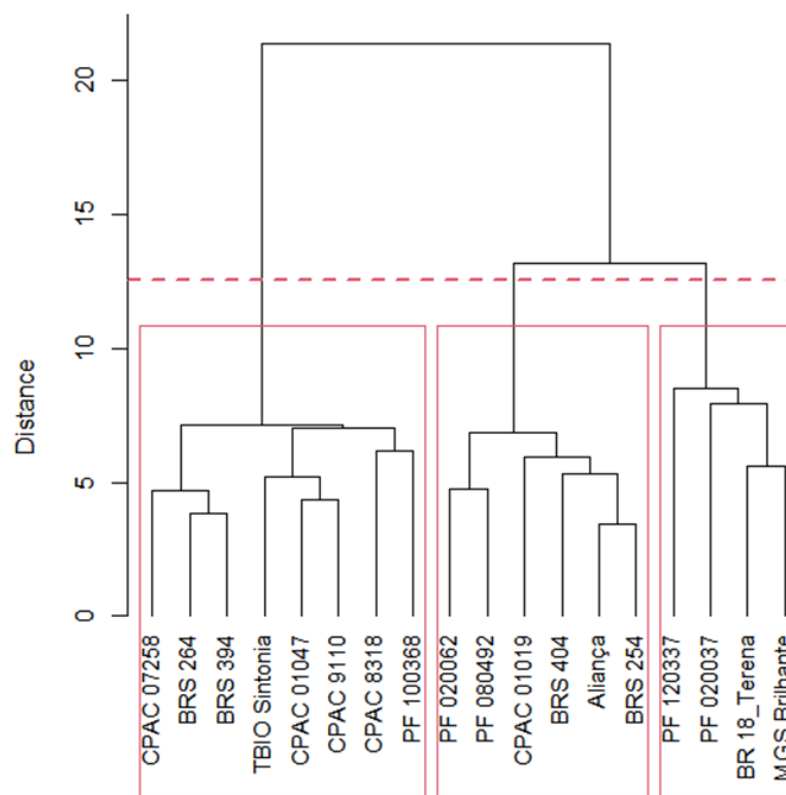


Figure 1. Dendrogram of eighteen wheat genotypes, based on Ward's clustering using the generalized Mahalanobis distance. Group 1: Aliança, BRS 254, BRS 404, CPAC 01019, PF 020062, and PF 080492; Group 2: BR 18_Terena, MGS Brilhante, PF 020037, and PF 120337; Group 3: BRS 264, BRS 394, CPAC 01047, CPAC 07258, CPAC 8318, CPAC 9110, PF 100368, and TBIO Sintonia.

The genotypes in Group 1 had a higher drought resistance index (DRI = 1.01) than the genotypes in Group 3 (DRI = 0.93), with intermediate values in Group 2 (DRI = 0.95) (Figure 2). Vegetative indices accounted for 97% of the total divergence observed among genotypes under water stress (Table 3). Indices based on the near-infrared band (OSAVI (33%), SAVI (33%), NDRE (11%), DVI (11%), GNDVI (3%), and NDVI (1%)) were most strongly associated with the differentiation of genotype groups. In addition, they were among the variables most affected by water stress.

Table 4. Relative importance (percentage) of variables for distance between genotypes according to Singh's (1981) [29] criterion.

Variables	Percentage (%)
SAVI	33
OSAVI	33
DVI	11
NDRE	11
GNDVI	3
NDGI	2
RVI	2
NDVI	1
GRVI	1

Table 4. Cont.

Variables	Percentage (%)
GY	1
Other	<2

SAVI: soil-adjusted vegetation index; OSAVI: optimized soil-adjusted vegetation index; DVI: difference vegetation index; NDRE: normalized difference red edge; GNDVI: green normalized difference vegetation index; NDGI: normalized differential greenness index; RVI: ratio vegetation index; NDVI: normalized difference vegetation index; GRVI: green red vegetation index; GY: grain yield.

Figure 2 shows the results of DRI (drought resistance index) for each group of wheat genotypes.

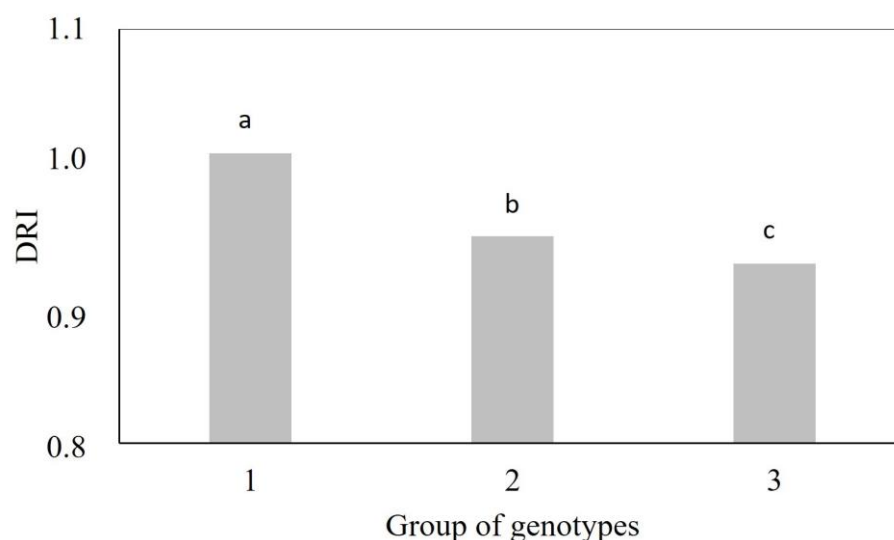


Figure 2. Drought resistance index (DRI) of groups of wheat genotypes. Group 1: Aliança, BRS 254, BRS 404, CPAC 01019, PF 020062, and PF 080492; Group 2: BR 18_Terena, MGS Brilhante, PF 020037, and PF 120337; Group 3: BRS 264, BRS 394, CPAC 01047, CPAC 07258, CPAC 8318, CPAC 9110, PF 100368, and TBIO Sintonia. Means followed by the same letter do not differ by the Tukey's test ($p < 0.05$).

The singular value decomposition of means of combinations of water regime levels and genotype groups retained 86% of the total variability in the first principal coordinate (Figure 3). However, there is a strong contrast in responses among genotype groups that received WR1 (22% of CET replacement) compared to the same groups with WR4 (100% of CET replacement). This means that the selection process must be carried out exactly under the conditions at the field, either under irrigation or under rainfed conditions.

The variable gas exchange (A , g_s and E) and vegetative indices (NDVI, GNDVI, GRVI, DVI, NDRE, SAVI, PRI, OSAVI, and TCARI) are correlated (Figures 3 and 4), and the higher correlations are between A and NDGI (0.78), g_s and RVI (0.73), and E and NDGI (0.70).

The variables $iWUE$, WUE , and R_m/S_m ratio positively correlate. In contrast, WUE and net CO_2 assimilation (A) negatively correlated (Figures 3 and 4). There are correlations between vegetative and gas exchange indices as they formed sharp angles between these variables, showing a correlation with grain yield, which should be the main criteria for the selection because yield is the most important variable.

All IVs except TCARI/OSAVI (TO) have a strong positive correlation (>0.6 , $p < 0.05$) with grain yield, photosynthetic rate, stomatal conductance, and transpiration (Figure 4). We observed correlations of 0.33 of total chlorophyll and 0.07 of root mass with grain yield, respectively. Mass of a thousand grains and grain yield are correlated (0.55). Negative correlations above 0.5 occur between these variables with WUE , $iWUE$, TO, and ratio

chlorophyll a to chlorophyll b. Positive correlations are observed between the WUE and iWUE variables ($0.3, p < 0.05$) (Figure 4).

Photosynthesis (A) and stomatal conductance (g_s) showed a high correlation with productivity (0.62 and 0.63 , respectively), but these evaluations can not be performed on a large scale. On the other hand, the vegetative indices TCARI, NDVI, OSAVI, SAVI, PRI, NDRE, and GNDVI showed the highest correlation with productivity ($>0.7, p < 0.05$). They can be useful in breeding programs (Figure 4) as they can be evaluated on a large scale. The vegetation indices were generally correlated, and not all of them need to be assessed for selecting wheat genotypes.

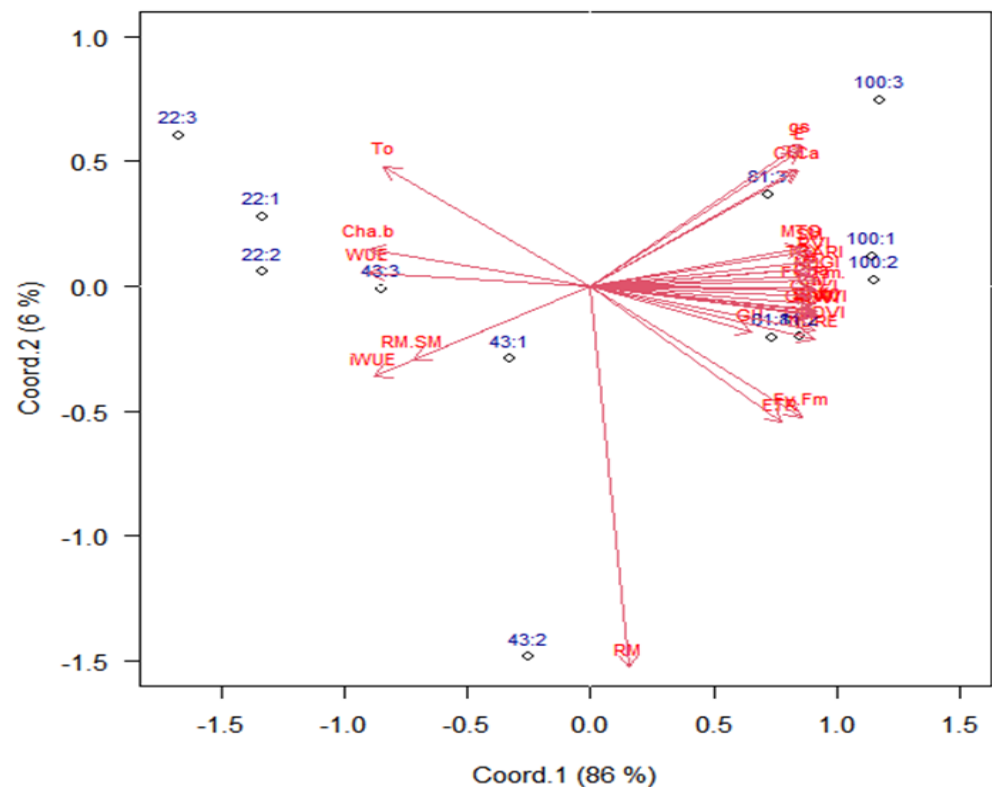


Figure 3. Biplot for scores of combined levels of water regimes (22, 43, 81, and 100% CET replacement, respectively) and wheat genotype groups (1, 2, and 3), based on the scores of principal coordinates from the variables: root mass (RM); shoot mass (SM); ratio RM/SM (RM.SM); grain humidity (GH); mass of thousand grain (MTG); grain yield (GY); water-use efficiency (WUE); intrinsic water-use efficiency (iWUE— A/g_s : net assimilation of CO_2 /stomatal conductance); transformed chlorophyll absorption and reflectance index (TCARI); green red vegetation index (GRVI); normalized difference vegetation index (NDVI); optimized soil-adjusted vegetation index (OSAVI); soil-adjusted vegetation index (SAVI); photochemical–physiological reflectance index (PRI); green normalized difference vegetation index (GNDVI); red edge normalized difference (NDRE); difference vegetation index (DVI); net assimilation of CO_2 (A); stomatal conductance (g_s); transpiration (E); internal CO_2 concentrations (C_i); electron transport rate (ETR); maximum quantum yield of photosystem II (F_v/F_m); effective quantum yield of photosystem (F_v'/F_m'); chlorophyll a (Cha); chlorophyll b (Chb); ratio chlorophyll a/b (Cha.b). Group 1: Aliança, BRS 254, BRS 404, CPAC 01019, PF 020062, and PF 080492; Group 2: BR 18_Terena, MGS Brilhante, PF 020037, and PF 120337; Group 3: BRS 264, BRS 394, CPAC 01047, CPAC 07258, CPAC 8318, CPAC 9110, PF 100368, and TBIO Sintonia.

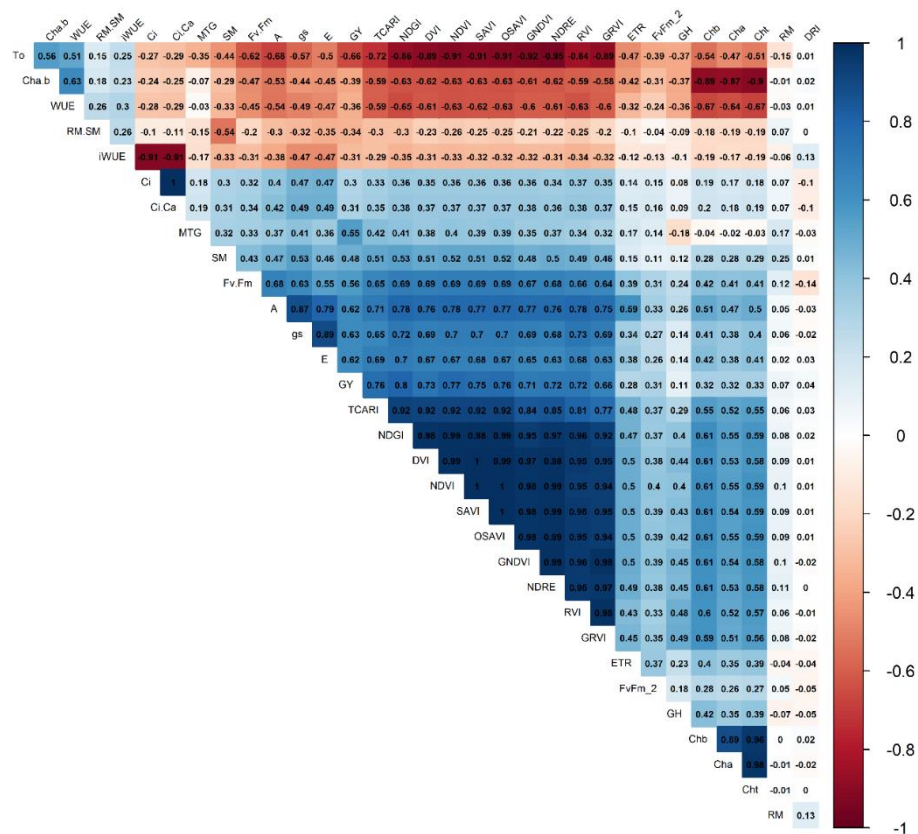


Figure 4. Pearson correlogram between variables representing physiological, spectral, and agronomic as a function of water regimes (22, 43, 81, and 100% CET replacement—WR1, WR2, WR3, and WR4, respectively) and wheat genotype groups (1, 2, and 3), based on the scores of principal coordinates from the variables: ratio RM/SM (RM.SM); ratio chlorophyll a/b (Cha.b); water-use efficiency (WUE); TCARI/OSAVI ratio (TO); intrinsic water-use efficiency (iWUE—A/gs: net assimilation of CO₂/stomatal conductance); electron transport rate (ETR)); maximum quantum yield of photosystem II (Fv/Fm); grain humidity (GH); chlorophyll b (Chb); chlorophyll a (Cha); chlorophyll b total (Cht); drought-resistance index (DRI); root mass (RM); internal CO₂ concentrations (Ci); mass of thousand-grain (MTG); shoot mass (SM); effective quantum yield of photosystem (Fv’/Fm’); stomatal conductance (gs); transpiration (E); grain yield (GY); net assimilation of CO₂ (A); the transformed chlorophyll absorption and reflectance index (TCARI); green red vegetation index (GRVI); normalized difference vegetation index (NDVI); optimized soil-adjusted vegetation index (OSAVI); soil-adjusted vegetation index (SAVI); photochemical–physiological reflectance index (PRI); green normalized difference vegetation index (GNDVI); red edge normalized difference (NDRE); difference vegetation index (DVI); normalized differential greenness index (NDGI); ratio vegetation index (RVI). Group 1: Aliança, BRS 254, BRS 404, CPAC 01019, PF 020062, and PF 080492; Group 2: BR 18_Terena, MGS Brilhante, PF 020037, and PF 120337; Group 3: BRS 264, BRS 394, CPAC 01047, CPAC 07258, CPAC 8318, CPAC 9110, PF 100368, and TBIO Sintonia.

Variables related to vegetative indices, gas exchange, chlorophyll, MTG, GY, WUE, and iWUE contents were the most important to differentiate genotype groups and water regime levels (Figure 3), as they have weights (length of arrows ($\cong 1.0$)) greater, indicating that these variables can be used to select wheat genotypes more productive under water stress and are also important components in the process of selecting more productive materials. Root mass (0–20 cm) had a low weight (0.25) for differentiating water regimes and genotype groups.

Without water stress, genotype groups with WR4 (100% of CET replacement) are mostly on the right side of the biplot, meaning that they present higher vegetative indices and photosynthetic activity, promoting higher grain yields (Figure 3).

The groups of genotypes showed linear positive responses of the latent variable (principal coordinate 1) (Table 5) as a function of the water regime. Additionally, we noticed that Group 3 has a response rate (slope = 0.0326) 18% higher on average. In contrast, the other two groups have similar slopes, probably because the genotypes grouped in three are classified as biotypes of irrigated crops, except for PF 100368 and TBIO Sintonia. The changes in water availability lead to significant changes in all traits according to the weights (horizontal arrow length) in the principal coordinate 1 (Figure 3).

Table 5. The regression equation for wheat variables as a function of water regime (x) for groups of genotypes.

Variable	Group of Genotype	Equation	R ²
Main Coordinate 1 (latent variable)	1	$y = -1.6339 + 0.0268x$	0.98
	2	$y = -1.4824 + 0.0266x$	0.98
	3	$y = -2.1757 + 0.0326x$	0.98
Grain Yield (kg ha ⁻¹)	1	$y = 5864.37 / (1 + \exp(-0.04 * (x - 31.3)))$	0.99
	2	$y = 5364.0 / (1 + \exp(-0.07 * (x - 29.36)))$	0.99
	3	$y = 6194.41 / (1 + \exp(-0.05 * (x - 31.32)))$	0.99
Net CO ₂ Assimilation (A, μmol CO ₂ m ⁻² s ⁻¹)	1	$y = 23.13 / (1 + \exp(-0.062 * (x - 30.24)))$	0.99
	2	$y = 23.18 / (1 + \exp(-0.047 * (x - 29.12)))$	0.99
	3	$y = 24.20 / (1 + \exp(-0.064 * (x - 32.53)))$	0.99
Normalized Difference Vegetation Index (NDVI)	1	$y = -0.52 + 0.2562 * \log(x)$	0.99
	2	$y = -0.46 + 0.2454 * \log(x)$	0.99
	3	$y = -0.62 + 0.2739 * \log(x)$	0.99
Water-use efficiency (WUE)	1	$y = 25.37 - 0.131 * \log(x)$	0.98
	2	$y = 23.22 - 0.109 * \log(x)$	0.99
	3	$y = 24.65 - 0.108 * \log(x)$	0.99
Intrinsic Water-use efficiency (iWUE)	1	$y = 135.88 - 0.846 * \log(x)$	0.96
	2	$y = 133.23 - 0.833 * \log(x)$	0.98
	3	$y = 126.47 - 0.824 * \log(x)$	0.97

Group 1: Aliança, BRS 254, BRS 404, CPAC 01019, PF 020062, and PF 080492; Group 2: BR 18 Terena, MGS Brilhante, PF 020037, and PF 120337; Group 3: BRS 264, BRS 394, CPAC 01047, CPAC 07258, CPAC 8318, CPAC 9110, PF 100368, and TBIO Sintonia. Water regime (WR1, WR2, WR3, and WR4—22, 43, 81, and 100% CET replacement, respectively).

3. Discussion

This paper studied the effect of four water regimes in twenty-seven variables and eighteen wheat genotypes. Through the joint multivariate analysis, we could separate the wheat genotypes into three groups (Tables 2 and 3) through genetic distance studies. This indicates that genetic variability in wheat genotypes among the studied variables is essential for conducting genetic distance studies (Figure 1). In addition, different responses to water regimes also occur among irrigated and rainfed wheat biotypes and other species, such as triticale and common beans [30].

The most similar genotypes were Aliança and BRS 254, and those that differed the most from PF 020037 and PF 120337. Aliança is a rainfed genotype and, in a previous study, was considered the most drought-tolerant genotype in severe water stress [2]. It is interesting to consider that rainfed and irrigated biotypes have distinct breeding programs conducted at different periods of the year. The irrigated biotype is cultivated in a more favorable climatic period for the species due to the cold at night and irrigated, which means a higher yield. In the target region (Cerrado), light is not a limiting factor in both planting periods.

Tavares et al. [31] studied six soybean genotypes in the Brazilian Cerrado region during the dry season and showed genotypes adapted to different water regimes.

The study carried out by Soares et al. [2] confirms the clustering results from this work, in which rainfed genotypes (Aliança, MGS Brilhante, and BRS 404) had higher DRI than

irrigated genotypes (BRS 394, BRS 254, and BRS 264) after two years of cultivation. This was expected since the genotypes classified in Group 1, except for CPAC 01019 and BRS 254, are rainfed biotypes. In contrast, the members of Group 3, except for genotypes PF 100368 and TBIO Sintonia, are biotypes for irrigated cultivation, which generally have a low DRI since they were developed for environments without water restriction. The wheat genotypes with higher DRI can be selected as a reference in breeding programs as they were more tolerant to water stress (Figure 2).

Using vegetative indices through cameras coupled in VANTS is a quick and non-invasive complementary method or can be replaced with the traditional selection of genotypes more tolerant to water stress [32–34].

Vegetative indices based on near-infra-red bands could separate the groups of wheat genotypes and were more affected by water stress, indicating the possibility of using vegetative indices as a quick and non-destructive way to differentiate and select wheat genotypes. Overall, these results are consistent with data from other authors who have found that NIR-based spectral indices have high accuracy and efficiency in selecting more productive wheat genotypes under water stress [28,35]. In contrast, indices based on the visible range correlate more strongly with plant growth [17,36].

In addition, spectral indices collected via cameras coupled to aircraft consistently show a stronger association with grain yield than indices obtained using proximal methods, indicating greater precision, speed, and scale gains [28].

Positive correlations of the NDVI, GNDVI, TCARI, and OSAVI vegetation indices and negative correlations between the TCARI/OSAVI index with shoot biomass and grain yield in wheat are reported by Frels et al. [37]. The TCARI/OSAVI index is very sensitive to chlorophyll variation and resistant to the effect of soil reflectance and non-photosynthetic matter, distorting the response in relation to the other index [38]. The non-destructive, simple, and fast measurement characteristics of PRI and NDRE constitute an important advantage over the physiological parameters (contents of photosynthetic pigments, chlorophyll fluorescence, and gas exchange rate). They will make it useful in stress detection, especially under severe levels or late stages of heat and water stress [39].

Genotypes under stressed conditions (WR1: 22% CET replacement) have higher values of WUE, iWUE, and TO (TCARI/OSAVI) (Tables 2 and 3) because there was less water lost, and TO, for instance, is a spectral predictor that is sensitive to chlorophyll variation [40].

The roots contribute only 10 to 20% of the total plant weight, but a well-developed root system is essential for the nutrition of nutrients and water and, therefore, for the growth and final yield of the plants [41] under conditions of limited water availability during vegetative growth, such as plants seeking to increase root volume to improve water uptake and avoid yield losses.

Water availability promoted significant alterations in all traits, according to the weights (horizontal arrow length) in the principal coordinate 1 (Figure 3). These observations confirm the findings of other authors who reported that under water deficit conditions, water relations and plant metabolism are impaired [15,42]. Photosynthesis can be affected by Rubisco activity and limited by chloroplast CO₂ concentration, i.e., under water deficit conditions, plants close stomata to prevent transpiration, which reduces photosynthesis by lowering CO₂ influx [14].

In addition to direct limitation, water stress can cause morphological changes in plants, such as changes in the organization of chloroplasts and the number of pigments, especially chlorophylls and xanthophylls, which consume energy and lead to lower grain yields [11,14]. Additionally, water stress reduces the number and length of the ears of wheat [2]. Abscisic acid (ABA) generally regulates and stimulates reactions such as stomata closure and maintaining water balance, and it stimulates transcription and activities of antioxidant enzymes under water deficit conditions [43].

In addition to drought tolerance, escape may occur because of some mechanism that prevents drought, including reduced leaf area, chlorophyll content, number of tillering, plant height, and stomatal conductance to avoid water loss; increased root length and root-

to-shoot ratio, probably to increase water uptake capacity; and increased proline content in leaves and reduce cycling [44]. Additionally, water stress reduced the plant cycle in our experiments, similar to Tavares et al. [31] working with soybeans.

Other studies show that water stress alters the morphology of the root system of wheat plants. For instance, changes in the root angle, primary root length, number of lateral roots [45], mean root diameter [46], and root mass [27] have been reported in the literature.

In the present study, with WR1 (22% CET replacement), a 31% reduction in shoot mass was observed in relation to the non-stressed water regime (WR4—100% CET replacement) (Table 3). A decrease in the shoot mass ratio and root mass suggests that wheat plants increase the root system to absorb more water. Furthermore, under a water deficit, wheat develops nodal roots with a narrower angle, which tend to grow deeper than those with a larger root angle and increase root density and decrease diameter; consequently, roots achieve deeper layers of soil [47].

The water regimes most affected the grain yield, net assimilation rate of CO₂, water-use efficiency, and NDVI (Figure 3). The groups of genotypes showed exponential responses of grain yield and net assimilation of CO₂ and a logarithm response of NDVI, water-use efficiency, and intrinsic water-use efficiency (Table 5).

Increasing water availability increased NDVI and photosynthetic activity, promoting higher grain yield. On a descending scale, we observed that genotypes of Groups 2 and 3 respond faster to water availability than genotypes of Group 1 for the variables grain yield, net CO₂ assimilation, and NDVI.

There is greater water-use efficiency under lower water availability. However, this efficiency is reduced more quickly in the genotypes of Groups 3 and 2 than in the genotypes of Group 1.

Soares et al. [2] also obtained differences between wheat genotypes for drought tolerance. The number of ears, the mass of a thousand grains, grain yield, net CO₂ assimilation, and hectoliter weight are important characteristics for selecting more productive genotypes. In addition, the variables DRI and water-use efficiency are important to classify genotypes for drought tolerance.

Water-use efficiency is a variable related to the ability of a plant to produce grains with a lower amount of water. Water-use efficiency by wheat plants increases under conditions of moderate water stress and decreases under stress-free conditions [11,12]. Using genotypes with greater water-use efficiency [48], especially for species with high water demand cultivated in rainfed agriculture [49], reduces crop losses in areas with water shortages.

4. Materials and Methods

4.1. Experimental Design and Conducting the Experiment

The study was carried out in the wheat cultivation areas in Planaltina, DF, Brazil (15°35'30" S and 47°42'30" W, an altitude of 1006 m) between May and September 2018 and 2019. The climate is classified as Aw (Koeppen–Geiger)—tropical, with rainfall concentrated in summer (October to April) and the dry period during the winter (May to September). The annual rainfall is between 1200 and 1500 mm. Precipitation and air temperature data from the experimental area in 2018 and 2019 are presented in Figure 5 and were obtained from a meteorological station close to the experiment. The experimental area had been cultivated for the last four years with wheat under different water regimes in winter and fallow in summer.

The soil is classified as Oxisol [50]. Before the installation of the experiment, soil samples were collected at a depth of 0–20 cm, with the following physicochemical properties: pH (CaCl₂) of 5.7, 11 mg dm⁻³ P (Mehlich–1), 186 mg dm⁻³, K 5.77 cmolc dm⁻³ Ca, 1.83 cmolc dm⁻³ Mg, 0.02 cmolc dm⁻³ Al, and 26.7 g kg⁻¹ organic matter. The soil texture comprised 46, 10, and 44% of clay, silt, and sand, respectively.

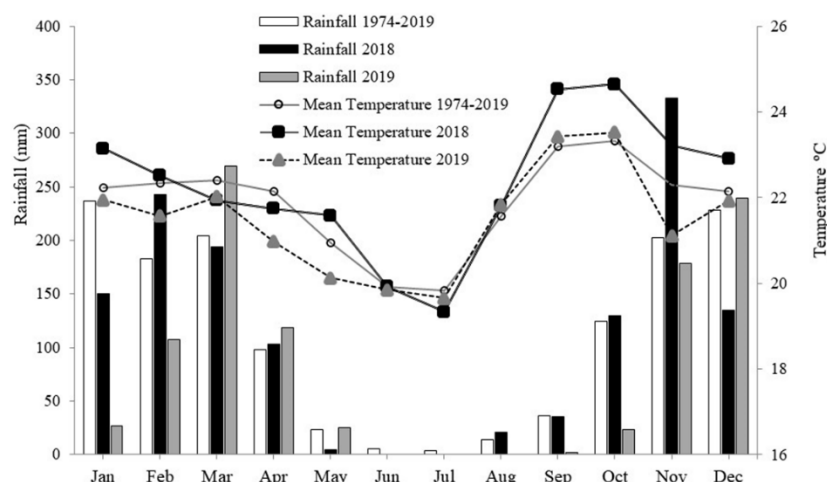


Figure 5. Precipitation and average temperature measured by an automatic weather station near the experiment in 2018 and 2019 and a historical series (1974–2019).

The model fitted the soil water retention curve [51]. The following estimates were obtained: residual water content (θ_s) $0.0839 \text{ cm}^3 \text{ cm}^{-3}$, saturated water content (θ_s) $0.5500 \text{ cm}^3 \text{ cm}^{-3}$, and parameters α (1.892 kPa^{-1}) and n (1.2390). The field capacity moisture was $0.3423 \text{ cm}^3 \text{ cm}^{-3}$.

Wheat biotypes developed for rainfed and irrigated planting periods were used, with different breeding improvement programs for the Cerrado region. The criterion for choosing the tested genotypes was to use recent and traditionally released materials and elite genotypes arising from the recent breeding program. The experiment was conducted in winter because there is almost no precipitation, which makes it easier to obtain an irrigation gradient.

The experimental design consisted of randomized blocks in a split-plot scheme with three replicates. The plots consisted of eighteen wheat genotypes: BRS 254, BRS 264, CPAC 01019, CPAC 01047, CPAC 07258, CPAC 08318, CPAC 9110, BRS 394 (irrigated biotypes) and Aliança, BR 18_Terena, BRS 404, MGS Brilhante, PF 020037, PF 020062, PF 120337, PF 100368, PF 080492, TBIO Sintonia (rainfed biotypes) all with similar cycle of approximately 110 days. Subplots were composed of four water regimes (WR). In 2018, 123.68 mm, 241.74 mm, 455.38 mm, and 562.2 mm were applied during the cycle, corresponding to WR1, WR2, WR3, and WR4, respectively. In 2019, 119.1 mm, 232.15 mm, 438.55 mm, and 541.43 mm were applied, corresponding to WR1, WR2, WR3, and WR4, respectively. In 2018 and 2019, the irrigation regimes used corresponded to 22%, 43%, 81%, and 100% of crop evapotranspiration (CET) replacement, respectively (Figure 6).

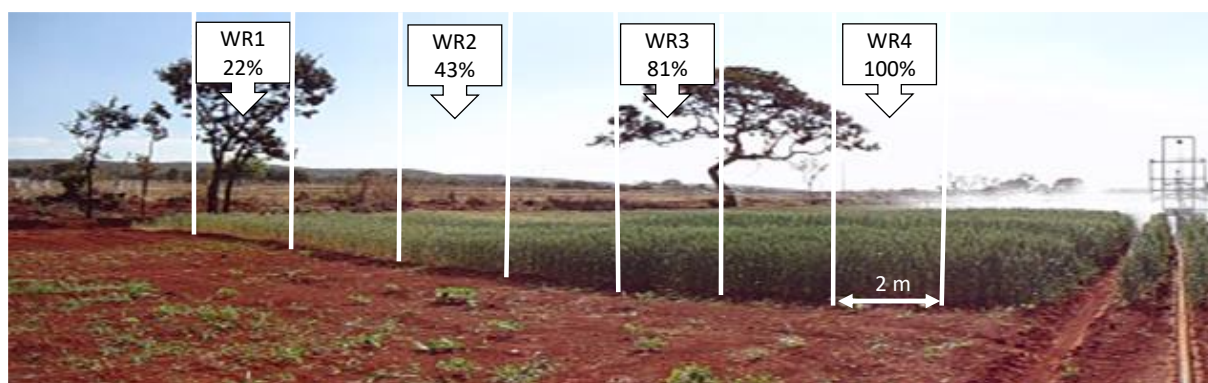


Figure 6. Graphical summary of experimental subunits (WR1, WR2, WR3 e WR4—22, 43, 81, 100% CET replacement, respectively) and the irrigation bar in wheat crop.

The rainfed biotypes were MGS Brillhante, Aliança, TBIO Sintonia, BR18_Terena (all traditional material), and BRS 404 (registered in 2014). The rainfed lines developed for the Cerrado region were PF020037 (strong wax formation on leaves and stems) and PF020062 (but without wax formation). In addition, the rainfed biotype PF080492 was adapted to the Brazilian Cerrado region [2]. The irrigated cultivars were BRS 254, BRS 264 (traditional materials), and BRS 394 (registered in 2014), and in the experimental phase for commercialization, the irrigated biotypes CPAC 01019, CPAC 01047, CPAC 07258, CPAC 08318, and CPAC 9110.

The highest-level irrigation was carried out according to the Cerrado Irrigation Monitoring Program [52], that is, by replacing evapotranspiration using regional agrometeorological indicators, soil texture, and date of total plant emergence date of the plants and estimating the reference evapotranspiration with based on the equation proposed by Penman-Monteith [53]. Irrigation was carried out approximately every five days, according to weather conditions and the phenological phase of the plants. The amount of water applied in each irrigation was estimated by collectors placed parallel to the irrigation bar.

Twenty days before planting, glyphosate was applied ($1440 \text{ g.e.a ha}^{-1}$). Seeding was done mechanically on 22 May 2018 and 23 May 2019 in a no-till system with 90 seeds per meter at a depth of 3 cm. Fertilization was carried in the furrows at 400 kg ha^{-1} of 04-30-16 (N, P_2O_5 , and K_2O), and at 25 days after wheat emergence (DAE), nitrogen was applied at a dose of 90 kg ha^{-1} N, as urea.

Furthermore, at 36 and 38 DAE, in 2018 and 2019, the growth reducer tranexamic-ethyl at a dose of 125 g ha^{-1} was applied in the first visible node and with the second palpable node. In addition, the herbicide metsulfuron-methyl was applied at 4 g ha^{-1} in both years for weed control on 15 DAE.

In both experiments, a homogeneous water layer was applied during the first 35 DAE at the tillering stage. An average of 150 mm of water was applied to obtain a homogeneous plant stand. After this period, the “line source” method was applied and modified by Jayme-Oliveira et al. [21]. The water regime (WR) was obtained by an irrigation bar (IrrigaBrasil model 36/42) 20 m wide on each side of the bar. The bar was connected to a self-propelled TurboMaq 75/GB) with controlled speed.

Each experimental unit consisted of a genotype with 18.0 m formed by eight cultivation rows spaced 0.17 m apart. Each water regime consisted of an experimental subunit 2.0 m in length formed by eight rows 0.17 m apart. The usable area consisted of the six central rows, omitting the margins and 2 m on each side.

4.2. Analyzed Variables

At the flowering stage (75 DAE), gas exchange and electron transport rate were evaluated from 8:30 am to 12:30 pm at an irradiance of $1200 \mu\text{mol photons m}^{-2}\text{s}^{-1}$ and an external CO_2 concentration (Ca) of $400 \mu\text{mol mol}^{-1}$. For each subplot, three fully expanded flag leaves were used to evaluate gas exchange using a portable open-flow gas exchange system (IRGA, model LI-6400xt LI-COR Inc., Lincoln, NE, USA). In addition, chlorophyll fluorescence and maximum quantum yield of photosystem II (Fv/Fm) were evaluated with a modulated portable fluorometer coupled to an IRGA. Evaluations were performed on dark-adapted leaves for at least three hours after 10:30 pm. During this period, initial fluorescence (F0), maximum fluorescence (Fm), and potential quantum yield of photosystem II ($\text{Fv/Fm} = (\text{F0} - \text{Fm})/\text{Fm}$) were estimated [54].

Chlorophyll a and b content were measured with the ClorofiLOG portable chlorophyll meter (CFL-1030, model Falker – Falker Agricultural Automation, Porto Alegre, Brazil), which provides relative measurements (0 to 100) of total chlorophyll but is linearly correlated with total chlorophyll content [55].

Using a multispectral camera, model Micasense RedEdge, which captures images in five different spectral ranges, that is, range: 465–485 nm; range: 550–570 nm; range: 663–673 nm; range: 712–722 nm; and range: 820–860 nm, coupled to an unmanned aerial vehicle (UAV) with a rotary wing, images were taken to estimate the vegetation indices in the

flowering phase of the crop. This camera features an optical resolution of 1280×960 pixels, with images recorded in RAW12 bits. The flight took place at a height of 45 m at 10 am. The reflectance maps were calculated by generating mosaics in the Pix4D Mapper software (v5.4.6, Pix4D, Lausanne, Switzerland).

The maps were processed in R software version 3.6.1 using the raster package, and the following vegetative indices were extracted as in Tavares et al. [31]: normalized difference vegetation index—NDVI; green normalized difference vegetation index—GNDVI; green-red vegetation index—GRVI; difference vegetation index—DVI; normalized difference red edge—NDRE; soil-adjusted vegetation index—SAVI; photochemical-physiological reflectance index—PRI; optimized soil-adjusted vegetation index—OSAVI; chlorophyll absorption and reflectance index—TCARI; TCARI/OSAVI—TO ratio.

Soil samples were collected to quantify the root mass of wheat genotypes during flowering. An auger with sharp edges, an internal diameter of 9.8 cm, and a length of 20 cm was used for root sampling. For each experimental subunit, 1508 cm³ of soil with roots was sampled, and the auger was inserted over the wheat crop line. The aerial part of the wheat plants corresponded to the area of the auger where the soil samples with roots (9.8 linear cm) were removed, cut close to the soil with a knife, and placed in a paper bag. The soil auger is made of stainless steel and has an iron shaft to facilitate rotation and application of force. This sampling procedure was adopted as in Ratke et al. [56].

The root samples with soil were kept in plastic bags, and the shoots in paper bags. The soil mass with roots was determined, and a subsample of 100 g was used to determine soil moisture content. Samples were stored in cold rooms at a temperature of -5 °C possible until the roots were separated from the soil to avoid loss of mass or drying the roots. Roots were separated from soil by washing with water three times in a 500 µm sieve and later separated from other organic materials. The roots and shoots were kept in a convection oven at 60 °C for 72 h to determine the dry matter. The results were expressed as root dry mass to soil mass ratio and root to shoot ratio.

At harvest, grain yield (GY) on the usable area of each experimental subunit and mass of thousand grains (MTG) was measured and standardized to the grain moisture content of 13% on a wet basis. Water-use efficiency (WUE) was calculated using the ratio of grain yield to crop water requirement [57]. The intrinsic water-use efficiency (iWUE) was calculated by the ratio between the net assimilation of CO₂ and stomatal conductance (A/g_s). The drought resistance index was calculated according to Fischer and Maurer [58].

4.3. Statistical Analysis

The data were subjected to joint multivariate analysis of variance by harvest based on singular value decomposition (SVD). Wheat genotypes were grouped based on the Mahalanobis distance using Ward's method. The Mojena criterion [59] was used to define the cutoff point in the dendrogram, and the relative importance (proportion) of variables in the distance between genotypes was determined by the Singh [29] criterion. In both years, treatments (combinations of genotypes and water regime levels) were analyzed graphically in a biplot [60]. This allows visualizing the relationship between genotypes and treatments. A Pearson correlation analysis (*t*-test, $p < 0.05$) was performed with the residuals. The statistical analyses were performed using the R v3.6.1. software.

5. Conclusions

High-throughput and non-destructive vegetative indices based on the near-infrared band can be used to detect drought tolerance of wheat genotypes, as they are correlated with physiological and agronomic traits. The wheat genotypes can be clustered according to their responses to water stress. The higher drought resistance index genotypes are Aliança, BRS 254, BRS 404, CPAC 01019, PF 020062, and PF 080492. On the other hand, the genotypes BRS 264, BRS 394, CPAC 01047, CPAC 07258, CPAC 8318, CPAC 9110, PF 100368, and TBIO Sintonia are the most affected by water availability. There is less variability in

wheat genotypes' physiological, agronomic, and spectral responses when providing water based on 100% evapotranspiration.

Author Contributions: Conceptualization: W.Q.R.J. and M.L.G.R.; methodology: W.Q.R.J., C.J.T., L.F.P., R.A.d.C.N.C. and C.A.F.d.S.; formal analysis: C.J.T., W.Q.R.J., M.L.G.R., A.R.d.S., O.M., L.F.P. and R.A.d.C.N.C.; investigation: W.Q.R.J., M.L.G.R., C.A.F.d.S. and L.F.P. writing and editing: W.Q.R.J., M.L.G.R., C.J.T., A.R.d.S., O.M. and A.R.d.S. All authors have read and agreed to the published version of the manuscript.

Funding: This paper was supported by the research group of Embrapa Cerrados, the University of Brasília, the Institute for Bio-and Geosciences (Julich), the Federal Institute Goiano, and this last institution released and supported the doctoral-level training of the first author.

Data Availability Statement: The data for this article can be shared upon reasonable request to the corresponding author.

Acknowledgments: The third and eight authors acknowledge the National Council for Scientific and Technological Development (CNPq) for the award for Excellence in Research.

Conflicts of Interest: The authors declare no conflict of interest.

References

- Soares, D.C.; Bonfim-Silva, E.M.; Silva, T.J.A.; Anicésio, E.C.A.; Duarte, T.F.; Oliveira, J.F. Growth and production of wheat cultivars under water tensions in Cerrado soil. *Rev. Bras. Eng. Agríc. Ambiental.* **2023**, *27*, 279–286. [CrossRef]
- Soares, G.F.; Ribeiro Júnior, W.Q.; Pereira, L.F.; Lima, C.A.; Soares, D.S.; Muller, O.; Rascher, U.; Ramos, M.L.G. Characterization of wheat genotypes for drought tolerance and water use efficiency. *Scient. Agricola.* **2021**, *78*, e20190304. [CrossRef]
- Pereira, J.F.; Cunha, G.R.; Moresco, E.R. Improved drought tolerance in wheat is required to unlock the production potential of the Brazilian Cerrado. *Crop. Breed. Appl. Biotechnol.* **2019**, *19*, 217–225. [CrossRef]
- Cattelan, A.J.; Dall'agnol, A. The rapid soybean growth in Brazil. *OCL* **2018**, *25*, D104. [CrossRef]
- Schauberger, B.; Rolinski, S.; Schaphoff, S.; Muller, C. Global historical soybean and wheat yield loss estimates from ozone pollution considering water and temperature as modifying effects. *Agric. For. Meteorol.* **2019**, *265*, 1–15. [CrossRef]
- Peña-Gallardo, M.; Vicente-Serrano, S.M.; Quiringb, S.; Svoboda, M.; Hannafordd, M.; Hannafordd, J.; Tomas-Burguera, M.; Martín-Hernández, N.; Domínguez-Castro, F.; Kenawy, E.A. Response of crop yield to different timescales of drought in the United States: Spatio-temporal patterns and climatic and environmental driver. *Agric. For. Meteorol.* **2019**, *264*, 40–55. [CrossRef]
- Conab. Companhia Nacional de Abastecimento. Acompanhamento da Safra Brasileira de Grãos. Safra 2022/2023, n. 1—Boletim de Monitoramento Agrícola—Cultivos de Verão e Inverno. 2023; pp. 1–20. Available online: <https://www.conab.gov.br/info-agro/safra/safra-graos/monitoramento-agricola> (accessed on 20 June 2023).
- Hatfield, J.L. Increased temperatures have dramatic effects on growth and grain yield of three maize hybrids. *Agric. Environ. Lett.* **2016**, *1*, 150006. [CrossRef]
- Wang, L.; Wang, S.; Chen, W.; Li, H.; Deng, X. Physiological mechanisms contributing to increased water-use efficiency in winter wheat under organic fertilization. *PLoS ONE* **2017**, *12*, e0180205. [CrossRef]
- Ahmed, H.G.M.-D.; Zeng, Y.; Yang, X.; Anwaar, H.A.; Mansha, M.Z.; Hanif, C.M.S.; Ikram, K.; Ullah, A.; Alghanem, S.M.S. Conferring drought-tolerant wheat genotypes through morpho-physiological and chlorophyll indices at seedling stage. *Saudi J. Biol. Sci.* **2020**, *27*, 2116–2123. [CrossRef]
- Pour-Aboughadareh, A.; Mohammadi, R.; Etmianan, A.; Shooshtari, L.; Maleki-Tabrizi, N.; Poczai, P. Effects of drought stress on some agronomic and morpho-physiological traits in Durum wheat genotypes. *Sustainability* **2020**, *12*, 5610. [CrossRef]
- Zhao, W.; Liu, L.; Shen, Q.; Yang, J.; Han, X.; Tian, F.; Wu, J. Effects of water stress on photosynthesis, yield, and water use efficiency in winter wheat. *Water* **2020**, *12*, 2127. [CrossRef]
- Anwaar, H.A.; Perveen, R.; Mansha, M.Z.; Abid, M.; Sarwar, M.; Aatif, H.M.; Umar, U.U.D.; Sajid, M.; Aslam, H.M.U.; Alam, M.M.; et al. Assessment of grain yield indices in response to drought stress in wheat (*Triticum aestivum* L.). *Saudi J. Biol. Sci.* **2020**, *27*, 1818–1823. [CrossRef] [PubMed]
- Ahmed, H.G.M.-D.; Sajjad, M.; Li, M.; Azmat, M.A.; Rizwan, M.; Maqsood, R.H.; Khan, S.H. Selection Criteria for Drought-Tolerant Bread Wheat Genotypes at Seedling Stage. *Sustainability* **2019**, *11*, 2584. [CrossRef]
- Ouyang, W.; Struik, P.C.; Yin, X.; Yang, J. Stomatal conductance, mesophyll conductance, and transpiration efficiency in relation to leaf anatomy in rice and wheat genotypes under drought. *J. Exp. Bot.* **2017**, *68*, 5191–5205. [CrossRef]
- Anderegg, J.; Yu, K.; Aasen, H.; Walter, A.; Liebisch, F.; Hund, A. Spectral vegetation indices to track senescence dynamics in diverse wheat germplasm. *Front. Plant Sci.* **2020**, *10*, 1749. [CrossRef] [PubMed]
- Yang, M.; Hassan, M.A.; Xu, K.; Zheng, C.; Rasheed, A.; Zhang, Y.; Jin, X.; Xia, X.; Xiao, Y.; He, Z. Assessment of water and nitrogen use efficiencies through uav-based multispectral phenotyping in winter wheat. *Front. Plant Sci.* **2020**, *11*, 927. [CrossRef] [PubMed]

18. El-Hendawy, S.E.; Al-Suhaibani, N.A.; Elsayed, S.; Hassan, W.M.; Dewir, Y.H.; Refay, Y.; Abdella, K.A. Potential of the existing and novel spectral reflectance indices for estimating the leaf water status and grain yield of spring wheat exposed to different irrigation rates. *Agri. Water Manag.* **2019**, *217*, 356–373. [[CrossRef](#)]
19. Munns, R.; James, R.A.; Sirault, X.R.; Furbank, R.T.; Jones, H.G. New phenotyping methods for screening wheat and barley for water stress tolerance. *J. Exp. Bot.* **2010**, *61*, 3499–3507. [[CrossRef](#)]
20. Qiu, R.C.; Wei, S.; Zhang, M.; Sun, H.; Li, H.; Liu, G.; Li, M. Sensors for measuring plant phenotyping: A review. *Int. J. Agric. Biol. Eng.* **2018**, *11*, 1–17. [[CrossRef](#)]
21. Jayme-Oliveira, A.; Ribeiro Junior, W.Q.; Ramos, M.L.G.; Ziviani, A.C.; Jakelaitis, A. Amaranth, quinoa, and millet growth and development under different water regimes in the Brazilian Cerrado. *Pesqui. Agropecu. Bras.* **2017**, *52*, 561–571. [[CrossRef](#)]
22. Fahlgren, N.; Gehan, M.A.; Baxter, I. Lights, camera, action: High-throughput plant phenotyping is ready for a close-up. *Curr. Opin. Plant Biol.* **2015**, *24*, 93–99. [[CrossRef](#)] [[PubMed](#)]
23. Sobejano-Paz, V.; Mikkelsen, T.N.; Baum, A.; Mo, X.; Liu, S.; Köppl, C.J.; Johnson, M.S.; Gulyas, L.; García, M. Hyperspectral and Thermal Sensing of Stomatal Conductance, Transpiration, and Photosynthesis for Soybean and Maize under Drought. *Remote Sens.* **2020**, *12*, 3182. [[CrossRef](#)]
24. Andrade-Sanchez, P.; Gore, M.A.; Heun, J.T.; Thorp, K.R.; Carmo-Silva, A.E.; French, A.N.; Salvucci, M.E.; White, J.W. Development and evaluation of a field-based high-throughput phenotyping platform. *Funct. Plant Biol.* **2014**, *41*, 68–79. [[CrossRef](#)] [[PubMed](#)]
25. Haghghattalab, A.; Gonzalez, L.; Mondal, S.; Singh, D.; Schinostock, D.; Rutkoski, J.; Ortiz-Monasterio, I.; Singh, R.; Goodin, D.; Poland, J. Application of unmanned aerial systems for high throughput phenotyping of large wheat breeding nurseries. *Plant Methods* **2016**, *12*, 35. [[CrossRef](#)] [[PubMed](#)]
26. Keller, B.; Vass, I.; Matsubara, S.; Paul, K.; Jedmowski, C.; Pieruschka, R.; Nedbal, L.; Rascher, U.; Muller, O. Maximum fluorescence and electron transport kinetics determined by light-induced fluorescence transients (LIFT) for photosynthesis phenotyping. *Photosynth. Res.* **2018**, *140*, 221–233. [[CrossRef](#)]
27. Khadka, K.; Earl, H.J.; Raizada, M.N.; Navabi, A. A Physio-Morphological Trait-Based Approach for Breeding Drought Tolerant Wheat. *Front. Plant Sci.* **2020**, *11*, 715. [[CrossRef](#)] [[PubMed](#)]
28. Hu, Y.; Knapp, S.; Schmidhalter, U. Advancing High-Throughput Phenotyping of Wheat in Early Selection Cycles. *Remote Sens.* **2020**, *12*, 574. [[CrossRef](#)]
29. Silva, A.D.N.; Ramos, M.L.G.; Ribeiro Junior, W.Q.; Alencar, E.R.; Silva, P.C.; Lima, C.A.; Vinson, C.C.; Silva, M.A.V. Water stress alters physical and Chemical quality ingrain of common bean, triticale and wheat. *Agri. Water Manag.* **2020**, *231*, 16023. [[CrossRef](#)]
30. Singh, D. The relative importance of characters affecting genetic divergence. *Indian J. Genet. Plant Breed.* **1981**, *41*, 237–245.
31. Tavares, C.J.; Ribeiro Junior, W.Q.; Ramos, M.L.G.; Pereira, L.F.; Casari, R.A.C.N.; Pereira, A.F.; de Sousa, C.A.F.; Silva, A.R.; Silva Neto, S.P.; Mertz-Henning, L.M. Water Stress Alters Morphophysiological, Grain Quality and Vegetation Indices of Soybean Cultivars. *Plants* **2022**, *11*, 559. [[CrossRef](#)]
32. Casari, R.A.C.N.; Paiva, D.S.; Silva, V.N.B.; Ferreira, T.M.M.; Souza, M.T.; Oliveira, N.G.; Kobayashi, A.; Molinari, H.B.C.; Santos, T.T.; Gomide, R.L.; et al. Using thermography to confirm genotypic variation for drought response in maize. *Int. J. Mol. Sci.* **2019**, *20*, 2273. [[CrossRef](#)] [[PubMed](#)]
33. Vitek, P.; Veselá, V.; Klem, K. Spatial and temporal variability of plant leaf responses cascade after PSII inhibition: Raman, chlorophyll fluorescence and infrared thermal imaging. *Sensors* **2020**, *20*, 1015. [[CrossRef](#)] [[PubMed](#)]
34. Silva, A.D.N.; Ramos, M.L.G.; Ribeiro Junior, W.Q.; da Silva, P.C.; Soares, G.F.; Casari, R.A.D.C.N.; Vinson, C.C. Use of Thermography to Evaluate Alternative Crops for Off-Season in the Cerrado Region. *Plants* **2023**, *12*, 2081. [[CrossRef](#)]
35. Bowman, B.; Chen, J.; Zhang, J.; Wheeler, J.; Wang, Y.; Zhao, W.; Nayak, S.; Heslot, N.; Bockelman, H.; Bonman, J. Evaluating grain yield in spring wheat with canopy spectral reflectance. *Crop Sci.* **2015**, *55*, 1881–1890. [[CrossRef](#)]
36. Prey, L.; Schmidhalter, U. Simulation of satellite reflectance data using high-frequency ground based hyperspectral canopy measurements for in-season estimation of grain yield and grain nitrogen status in winter wheat. *ISPRS J. Photogramm. Remot.* **2019**, *149*, 176–187. [[CrossRef](#)]
37. Frels, K.; Guttieri, M.; Joyce, B.; Leavitt, B.; Baenziger, P.S. Evaluating canopy spectral reflectance vegetation indices to estimate nitrogen use traits in hard winter wheat. *Field Crops Res.* **2018**, *217*, 82–92. [[CrossRef](#)]
38. Damm, A.; Paul-Limoges, E.; Haghghi, E.; Simmer, C.; Morsdorf, F.; Schneider, F.D.; Van Der Tol, C.; Migliavacca, M.; Rascher, U. Remote sensing of plant-water relations, An overview and future perspectives. *J. Plant Physiol.* **2018**, *227*, 3–19. [[CrossRef](#)]
39. Cao, Z.; Yao, X.; Liu, H.; Liu, B.; Cheng, T.; Tian, Y.; Cao, W.; Zhu, Y. Comparison of the abilities of vegetation indices and photosynthetic parameters to detect heat stress in wheat. *Agri. For. Meteorol.* **2019**, *265*, 121–136. [[CrossRef](#)]
40. Ballester, C.; Zarco-Tejada, P.J.; Nicolás, E.; Alarcón, J.J.; Fereres, E.; Intrigliolo, D.S.; Gonzalez-Dugo, V. Evaluating the performance of xanthophyll, chlorophyll and structure-sensitive spectral indices to detect water stress in five fruit tree species. *Precis. Agric.* **2018**, *19*, 178–193. [[CrossRef](#)]
41. Liu, W.; Wang, J.; Wang, C.; Ma, G.; Wei, Q.; Lu, H.; Xie, Y.; Ma, D.; Kang, G. Root growth, water and nitrogen use efficiencies in winter wheat under different irrigation and nitrogen regimes in North China Plain. *Front. Plant Sci.* **2018**, *9*, 1798. [[CrossRef](#)]
42. Marček, T.; Hamow, K.; Vég, B.; Janda, T.; Darko, E. Metabolic response to drought in six winter wheat genotypes. *PLoS ONE* **2019**, *14*, e0212411. [[CrossRef](#)] [[PubMed](#)]

43. Wang, X.; Li, Q.; Xie, J.; Huang, M.; Cai, J.; Zhou, Q.; Dai, T.; Jiang, D. Abscisic acid and jasmonic acid are involved in drought priming-induced tolerance to drought in wheat. *Crop J.* **2021**, *9*, 120–132. [[CrossRef](#)]
44. Li, P.; Ma, B.; Palta, J.A.; Ding, T.; Cheng, Z.; Lv, G.; Xiong, X. Wheat breeding highlights drought tolerance while ignores the advantages of drought avoidance: A meta-analysis. *Eur. J. Agron.* **2021**, *122*, 126196. [[CrossRef](#)]
45. Zhan, A.; Lynch, J.P. Reduced frequency of lateral root branching improves N capture from low-N soils in maize. *J. Exp. Bot.* **2015**, *66*, 2055–2065. [[CrossRef](#)]
46. Haling, R.E.; Brown, L.K.; Bengough, A.G.; Young, I.M.; Hallett, P.D.; White, P.J. Root hairs improve root penetration, root–Soil contact, and phosphorus acquisition in soils of different strength. *J. Exp. Bot.* **2013**, *64*, 3711–3721. [[CrossRef](#)] [[PubMed](#)]
47. Chen, X.; Ding, Q.; Błazzkiewicz, Z.; Sun, J.; Sun, Q.; He, R.; Li, Y. Phenotyping for the dynamics of field wheat root system architecture. *Sci. Rep.* **2017**, *7*, 37649. [[CrossRef](#)]
48. Yasi, H.; Attia, H.; Alamer, K.; Hassan, F.; Ali, E.; Elshazly, S.; Siddique, K.H.M.; Hessini, K. Impact of drought on growth, photosynthesis, osmotic adjustment, and cell wall elasticity in Damask rose. *Plant Physiol. Biochem.* **2020**, *150*, 133–139. [[CrossRef](#)] [[PubMed](#)]
49. Tavera, V.C.; Mancilla, C.L.A.; Gallegos, J.A.C.; Pimentel, J.G.R.; Arriaga, A.I.M.; Ruiz Nietto, J.E. Mechanisms for water use efficiency between bean cultivars tolerant to drought are different. *Acta Sci. Agron.* **2018**, *40*, e39378. [[CrossRef](#)]
50. Soil Survey Staff. Keys to Soil Taxonomy. In *Soil Survey Field and Laboratory Methods Manual. Soil Survey Investigations Report, No. 51, Version 2.0*; Burt, R., Soil Survey Staff, Eds.; U.S. Department of Agriculture, Natural Resources Conservation Service: Washington, DC, USA, 2014.
51. Van Genuchten, M.T. A closed-form equation for predicting the hydraulic conductivity of unsaturated soils. *Soil Sci. Soc. Am. J.* **1980**, *44*, 892–898. [[CrossRef](#)]
52. Embrapa. *Programa de Monitoramento da Irrigação*; EMBRAPA: Brasília, Brazil, 2011.
53. Allen, R.G.; Pereira, L.S.; Raes, D.; Smith, M. Crop evapotranspiration: Guidelines for computing crop water requirements. *FAO Irrig. Drain. Pap.* **1998**, *56*, 300.
54. Genty, B.; Briantais, J.M.; Baker, N.R. The relationship between the quantum yield of photosynthetic electron transport and quenching of chlorophyll fluorescence. *Biochim. Biophys. Acta* **1989**, *990*, 87–92. [[CrossRef](#)]
55. Rigon, J.P.G.; Capuani, S.; Beltrão, N.M.; Brito Neto, J.F.; Sofiatti, V.; França, V.F. Non-destructive determination of photosynthetic pigments in the leaves of castor oil plants. *Acta Sci. Agron.* **2012**, *34*, 325–329. [[CrossRef](#)]
56. Ratke, R.F.; Pereira, H.S.; Santos Junior, D.G.; Frazão, J.J.; Barbosa, J.M.; Dias, B.O. Root growth, nutrition and yield of maize with applied different limestone particle size in the cerrado soil. *Am. J. Plant Sci.* **2014**, *5*, 463–472. [[CrossRef](#)]
57. Hatfield, J.L.; Sauer, T.J.; Prueger, J.H. Managing soils to achieve greater water use efficiency: A review. *Agronomy* **2001**, *93*, 271–280. [[CrossRef](#)]
58. Fischer, R.A.; Maurer, R. Drought resistance in spring wheat cultivars. I. Grain yield responses. *Aust. J. Agric. Res.* **1978**, *29*, 897–912. [[CrossRef](#)]
59. Mojena, R. Hierarchical grouping methods and stopping rules: An evaluation. *J. Comput.* **1977**, *20*, 359–363. [[CrossRef](#)]
60. Gabriel, K.R. The biplot graphical display of matrices with application to principal component analysis. *Biometrika* **1971**, *58*, 453–467. [[CrossRef](#)]

Disclaimer/Publisher’s Note: The statements, opinions and data contained in all publications are solely those of the individual author(s) and contributor(s) and not of MDPI and/or the editor(s). MDPI and/or the editor(s) disclaim responsibility for any injury to people or property resulting from any ideas, methods, instructions or products referred to in the content.